

A modular clamp-like mechanism to regulate the activity of nucleic-acid target-responsive nanoswitches with external activators

Erica Del Grosso¹, Andrea Idili¹, Alessandro Porchetta¹ and Francesco Ricci^{1*}

¹Dipartimento di Scienze e Tecnologie Chimiche, University of Rome, Tor Vergata, Via della Ricerca Scientifica, 00133, Rome, Italy; *Corresponding author: francesco.ricci@uniroma2.it

Supporting information

Reagents

Reagent-grade chemicals, including disodium phosphate, monosodium phosphate, tris-(2-carboxyethyl) phosphine hydrochloride, magnesium chloride, adenosine 5'-triphosphate (ATP) disodium salt hydrate, gentamicin solution and cocaine (all from Sigma-Aldrich, St Louis, Missouri) were used without further purifications.

HPLC purified DNA-oligonucleotides modified with 6-carboxyfluorescein (6-FAM) and a quencher (Black Hole Quencher 1, BHQ-1) were purchased from Biosearch Technologies (Risskov, Denmark) and from IBA (Gottingen, Germany) and employed without further purification.

Oligonucleotide sequences

Below are reported the oligonucleotide sequences for all the modulators designed in this work. For all the sequences given below the underlined bases represent the portion of the split target-responsive module (see Figure 1, red portion) and italics bases represent the control module (see Figure 1, green portion) and the bold bases the random linker.

Clamp-like regulated nucleic acid nanoswitch based on a triplex-forming portion as the control module and an ATP-binding split aptamer as the target-responsive module (Figure 1C):

Optically-labeled clamp-like nanoswitch (random loop of 20 thymines):

5'-(FAM)-ACCTGGGGGAGTA-TGA-*CTCTCTCTTTT*-**TTTTTTTTTTTTTTTTTTTTTTT**-*TTTTCTTCTCTC*-TGA-TGCGGAGGAAGGA-(BHQ1)-3'

Perfect match activator: (10 bases): 5'-*AAA AGA AGA G*-3'

Mismatch activator (10 bases): 5'-*AAA ATA AGA G*-3'

Strand used to demonstrate the reversibility (Figure 2A).

Activator with a toehold of 10 bases: 5'- TCA TAG AGT C – *AAA AGA AGA G*-3'

Competitor: 5'- *CTC TTC TTT T* – GAC TCT ATG A-3'

Clamp-like regulated nucleic acid nanoswitch with a split ATP-binding aptamer as the control module and the triplex-forming portion as the target-responsive module (Figure 3A):

Optically-labeled clamp-like nanoswitch (random loop of 30 thymines):

5'-(FAM)-ATTTTCTTCTC-TGA-*CCTGGGGGAGTAT*-TTT-*TGCGGAGGAAGG*-TGA-CTCTTCTTTTA-(BHQ1)-3'

Optically-labeled clamp-like nanoswitch (random loop of 8 thymines):

5'-(FAM)-ATTTTCTTCTC-TGA-*CCTGGGGGAGTAT*-TTTTTTTTT-*TGCGGAGGAAGG*-TGA-CTCTTCTTTTA-(BHQ1)-3'

DNA-target (10 bases): 5'-AAA AGA AGA G-3'

Clamp-like regulated nucleic acid nanoswitch with a split cocaine-binding aptamer as the control module and the triplex-forming portion as the target-responsive module (Figure 3E):

Optically-labeled clamp-like nanoswitch (random loop of 30 thymines):

5'-(FAM)-ACTCCTTCTC-AT-*GAGAACAAGGAAAA*-TTT-*TCCTTCAATGAAGTGGGTCGA*-TA-CTCTTCCTCA-(BHQ1) - 3'

DNA-target (9 bases) : 5'-GAG GAA GAG-3'

Clamp-like regulated nucleic acid receptor with a split gentamicin-binding aptamer as the control module and the triplex-forming portion as the target-responsive module (Figure 3F):

Optically-labeled clamp-like nanoswitch (random loop of 30 thymines):

5'-(FAM)-ACTTTCTTCT-TGA-*CTTGG*-TTT-*AGGTAATGAG*-TGA-TCTTCTTTCA-(BHQ1)-3'

DNA-target (9 bases): 5'-AGA AGA AAG-3'

Clamp-like regulated nucleic acid nanoswitch based on two triplex-forming recognition modules as both control and target-responsive modules (Figure 4A):

Optically-labeled clamp-like nanoswitch:

5'-(FAM)-ACCTTCTCTCC-AGT-TCTTCTTTC-AGTTATTATTAGTTATTATT-CTTTTCTTCT-TGA-CCTCTCTTCCA-(BHQ1)- 3'

Perfect match activator: (10 bases): 5' - *AGA AGA AAA G* - 3'

Mismatch activator (10 bases): 5' - *AGA ATA AAA G*-3'

DNA-target (10 bases): 5' - GGA AGA GAG G -3'

Strand used to demonstrate the reversibility (Figure S9).

Activator with a toehold of 10 bases: 5' - *AGA AGA AAA G* – TCA TAG AGT C-3'

Competitor: 5' - GAC TCT ATG A – *CTT TTC TTC T*-3'

Buffer conditions

All oligonucleotides were suspended to a final concentration of 100 μ M in phosphate buffer 50 mM, pH 7 and stored at -20°C.

Binding curves

Fluorescence measurements were obtained using a Cary Eclipse Fluorometer (Varian) or a fluorometer microplate-reader, Tecan Infinite M200pro (Männedorf, Switzerland), with an excitation at 495 nm (\pm 5 nm) and emission at 520 nm (\pm 5 nm). Measurements were performed in a 100 mM Tris buffer + 10 mM MgCl₂, pH 7.4, 25°C. Only for the cocaine-regulated nanoswitch we used a 100 mM Tris buffer, pH 7.4 without the addition of MgCl₂.

Binding curves were obtained using a fixed concentration of the clamp-like regulated nanoswitch (10⁻⁸ M) and by adding increasing concentrations of the target. The resulting fluorescent signals were fitted using the following Langmuir equation to obtain K_D values:

Eq. 1

$$F(T) = F_0 + \left(\frac{[T](F_B - F_0)}{[T] + K_D} \right)$$

Where $F(T)$ is the fluorescence in presence of different concentration of target, F_0 is the background fluorescence, $[T]$ is the target concentration, F_B is the fluorescence in presence of saturating concentration of target.

Correlation between theoretical and experimental K_D

The experimentally obtained values of K_D for each clamp-like regulated nanoswitch have been compared with the values predicted by the allosteric model (see Eq. 1 in the text and eq. 2 below). The simulated K_D values can be easily obtained using the following equation:

Eq. 2

$$K_D = K_D^{No\,eff} \left(\frac{1 + \frac{[Eff]}{K_{eff}}}{1 + \frac{[Eff]}{\alpha K_{eff}}} \right)$$

where K_{eff} is the dissociation constant between the activator and the clamp-like regulated nanoswitch, α is the ratio between the target dissociation constants in the presence of saturating activator concentration and in the absence of activator (K_D^{no-eff}).

Times-course experiments

Time-course experiments were obtained using a Cary Eclipse Fluorometer (Varian) with an excitation at 495 nm (± 5 nm) and emission at 520 nm (± 5 nm). Measurements were performed in 100 mM Tris buffer + 10 mM $MgCl_2$, pH 7.4, 25°C, using a fixed concentration of the clamp-like regulated nanoswitch (10^{-8} M). After reaching a stable baseline (5 minutes) we added the target to a solution with or without the activator. For the clamp-like regulated nucleic acid nanoswitch with a split ATP-binding aptamer as the target-responsive module (Figure 1D) we used a final concentration of 3×10^{-7} M for the activator and 5×10^{-5} M for ATP. For the clamp-like regulated nucleic acid nanoswitch with a split ATP-binding aptamer as the control module (Figure 3B) we used a final concentration of 7×10^{-4} M for the ATP and 5×10^{-8} M for the target. For the clamp-like regulated nucleic acid nanoswitch based on

two triplex-forming recognition modules (Figure 4B) we used a final concentration of 3×10^{-7} M for the activator and 5×10^{-9} M for the target.

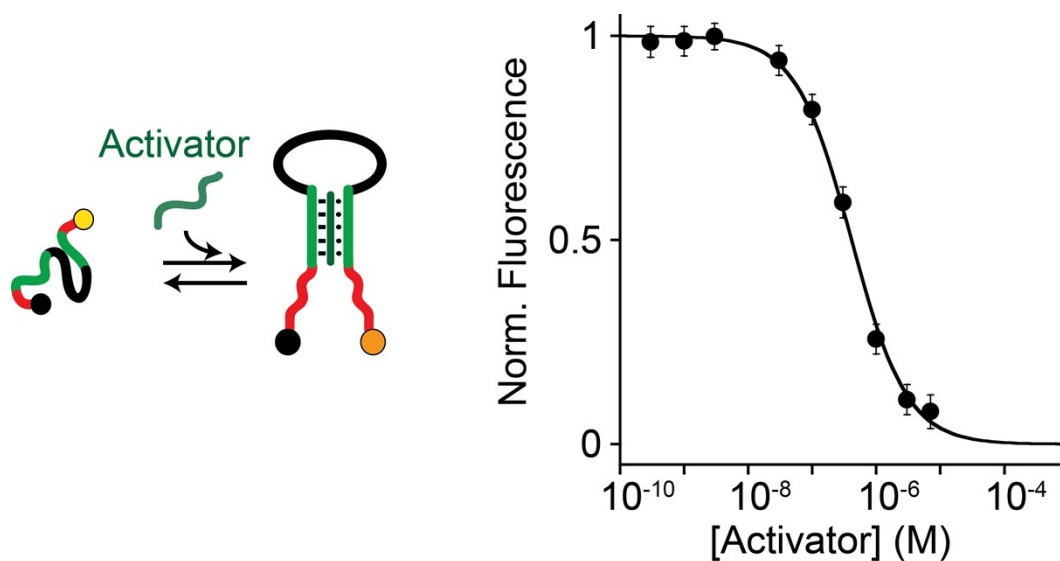


Figure S1. Binding curve of the activator for the clamp-like regulated nucleic acid nanoswitch based on a triplex-forming recognition control module and an ATP-binding split aptamer (Figure 1C). From this binding curve it is possible to estimate the dissociation constant of the clamp-like nanoswitch for the activator (K_{eff}) and use this value for simulation purposes (Figure 1F, solid line).

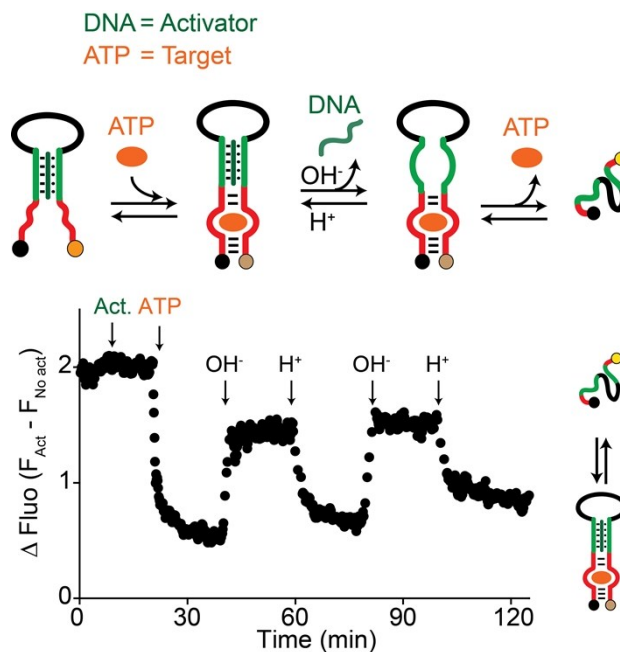


Figure S2. Reversible load and release of ATP. Because the binding of the activator to the clamp-like nanoswitch involves the formation of pH-dependent Hoogsteen interactions we can regulate the activation of the nanoswitch by changing the solution's pH. For example, by cyclically varying the pH of a solution containing the activator (10^{-7} M) and ATP (5×10^{-5} M) it is possible to bind (low pH) or release (high pH) the activator from the nanoswitch. As a consequence, the binding ability of the nanoswitch towards ATP can be activated or inhibited respectively and ATP can be loaded and released in a reversible way. Here ATP binding to the clamp-like nanoswitch is followed by time-course fluorescence measurements obtained in a solution of nanoswitch (10^{-8} M) in a 100 mM Tris buffer + 10 mM MgCl_2 , pH 7.0, 25°C. After a stable baseline was obtained the activator was added and after the further stabilization of the baseline ATP was added. The addition of a small aliquot of 1 M NaOH was used to reach a pH of 7.4 while the addition of a small aliquot of 1 M HCl was used to reach a pH of 7.0.

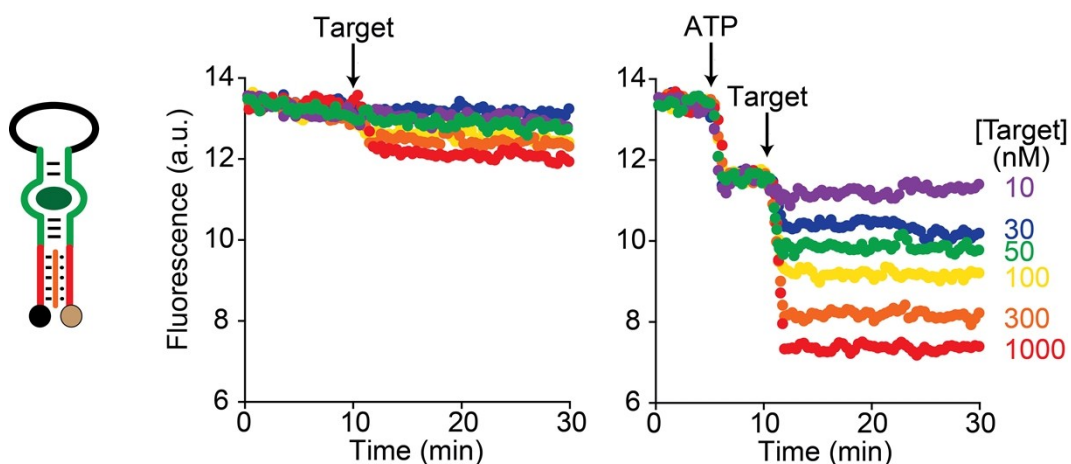


Figure S3. DNA binding activity of our clamp-like regulated nucleic acid nanoswitch with a split ATP-binding aptamer as the control module (Figure 3A) can be easily restored in the presence of the activator (ATP). Here DNA target binding to the clamp-like nanoswitch is followed by time-course fluorescence measurements obtained in a solution of nanoswitch (10^{-8} M) in a 100 mM Tris buffer + 10 mM MgCl_2 , pH 7.4, 25°C. After a stable baseline was obtained the DNA target was added (where indicated by the arrow) at the indicated concentrations. Colours code concentration of the left figure is the same of the right figure. Only in the presence of ATP (7×10^{-4} M, right) the nanoswitch ability to bind the DNA target is restored.

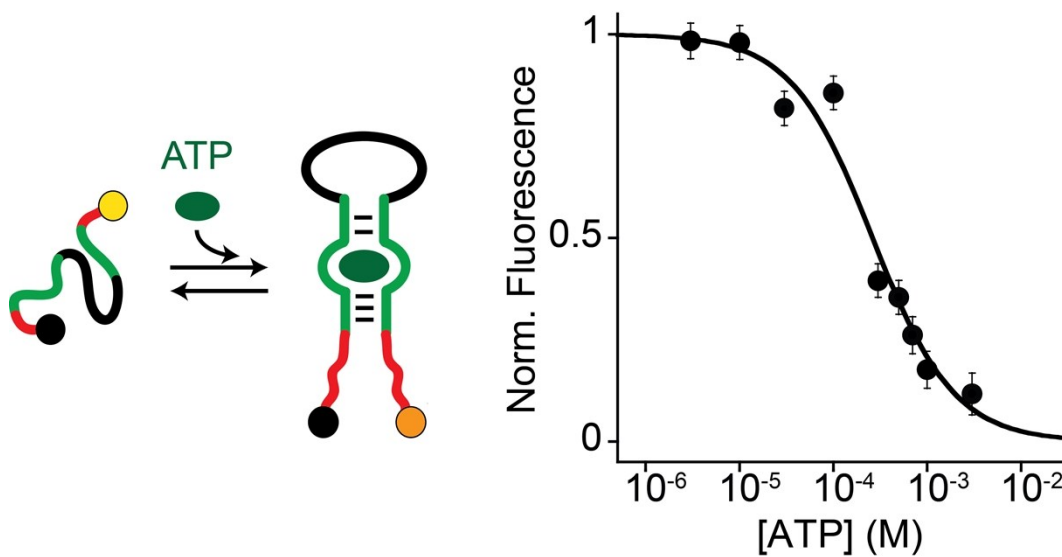


Figure S4. Binding curve of the ATP for the clamp-like regulated nucleic acid nanoswitch with a split ATP-binding aptamer as the control module and the triplex-forming portion as the target-responsive module (Figure 3A). From this binding curve it is possible to estimate the dissociation constant of the nanoswitch for the modulator (K_{eff}) and use this value for simulation purposes (Figure 3D, solid line).

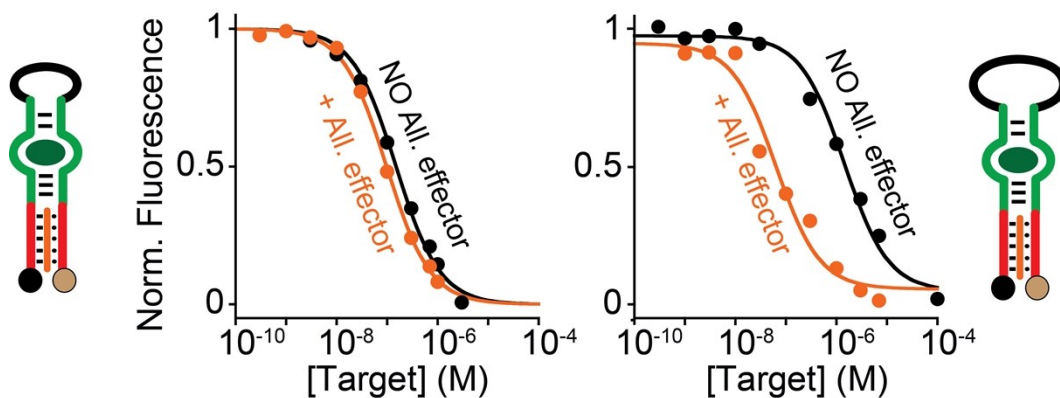


Figure S5. Effect of linker length on the control behavior of our nanoswitch. Here we tested clamp-like regulated nucleic acid nanoswitch with a split ATP-binding aptamer as the control module and the triplex-forming portion as the target-responsive module (Figure 3A) with two different lengths of the linker (8 bases, left and 30 bases, right). As expected, because a shorter linker does not provide enough entropic disorder, the resulting nanoswitch is only partially regulated by ATP (left). Only with a longer linker we can observe efficient control of our nanoswitch (right).

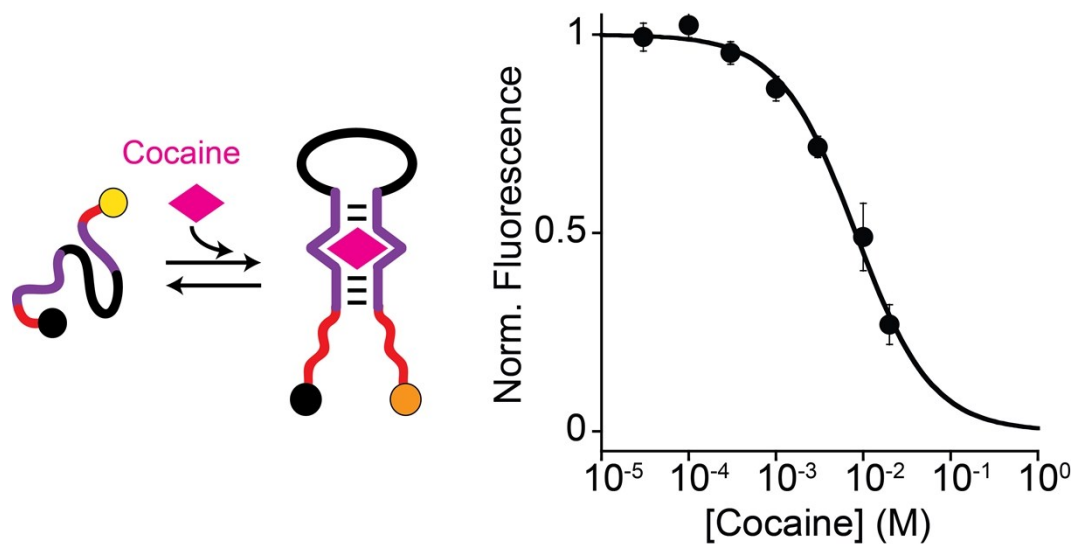


Figure S6. Binding curve of the Cocaine for the clamp-like regulated nucleic acid nanoswitch with a split cocaine-binding aptamer as the control module and the triplex-forming portion as the target-responsive module (Figure 3E).

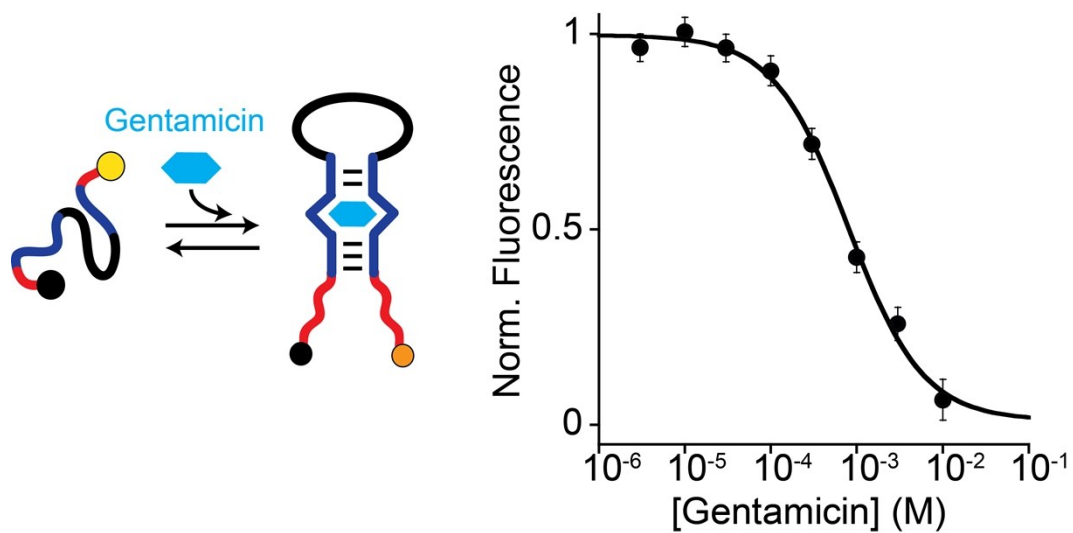


Figure S7. Binding curve of the Gentamicin for the clamp-like regulated nucleic acid nanoswitch with a split gentamicin-binding aptamer as the control module and the triplex-forming portion as the target-responsive module (Figure 3F).

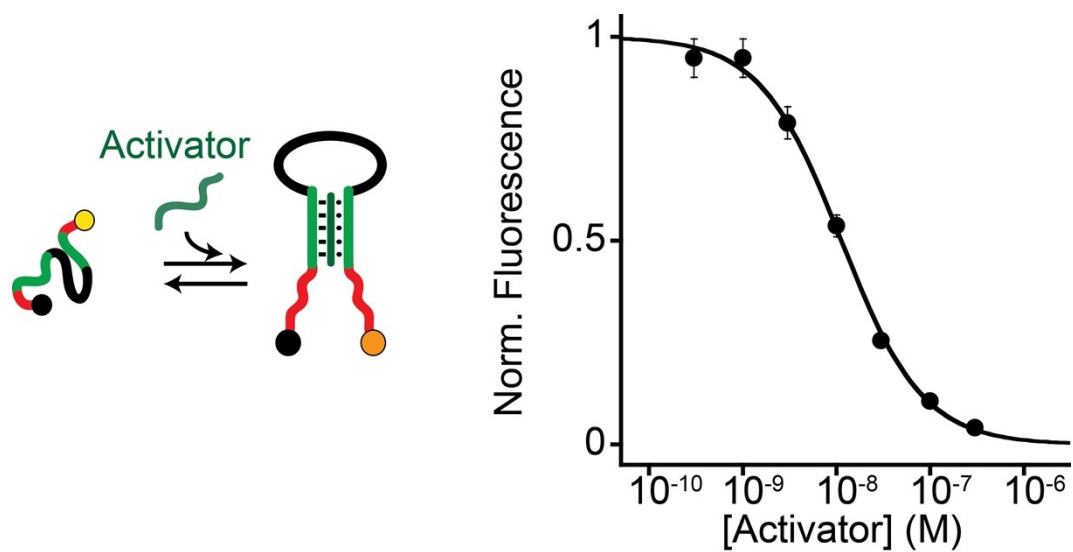


Figure S8. Binding curve of the activator for the clamp-like regulated nucleic acid nanoswitch based on two triplex-forming recognition modules as both control and target-responsive modules (Figure 4A). From this binding curve it is possible to estimate the dissociation constant of the nanoswitch for the modulator (K_{eff}) and use this value for simulation purposes (Figure 4D, solid line).

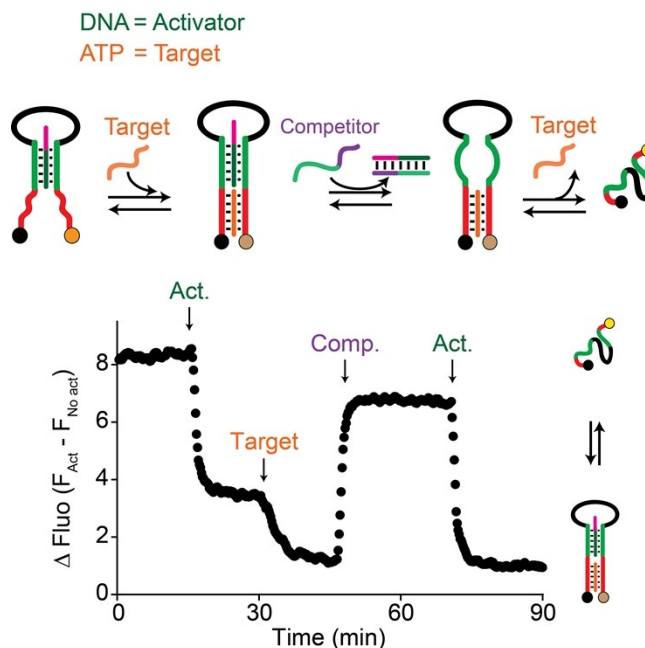


Figure S9. (Top) The clamp-like nanoswitch containing two DNA recognizing binding sites is reversible. In a way similar to that showed for the DNA/ATP nanoswitch (see Figure 2) we used here a DNA-activator with a toehold of 10 bases that can be removed by a complementary competitor. (Bottom) In the presence of the activator the nanoswitch partially folds restoring binding activity for the DNA target. By adding the competitor it is possible to selectively displace the activator. This, in turn, leads to the release of the DNA target from the nanoswitch. Here the DNA target loading/release to the clamp-like nanoswitch is followed by time-course fluorescence measurements obtained in a solution of nanoswitch (10^{-8} M) in a 100 mM Tris buffer + 10 mM MgCl_2 , pH 7.4, 25°C with the injection of the activator (10^{-7} M), target DNA (10^{-8} M) and competitor (2×10^{-6} M).